

# Characterization of solar selective molybdenum black films

H. S. POTDAR, A. B. MANDALE, S. D. SATHAYE, A. P. B. SINHA  
*Physical Chemistry Division, National Chemical Laboratory, Pune 411 008, India*

It has been found possible to prepare excellent solar selective molybdenum black films by a modified cathodic electrodeposition technique. These films have been characterized using XPS, AES depth profiling, SEM, chemical analysis, X-ray diffraction and VIS-IR reflectance spectroscopy. The study shows that the film is composite of  $\text{MoO}_3$  matrix containing fine nickel and copper particles. It is also observed that the copper concentration increases from the surface of the film towards the substrate. Reported solar selectivity can be explained using the Maxwell Garnett theory along with the stacked layer treatment developed by Anderson.

## 1. Introduction

The required spectral selectivity for efficient photo-thermal conversion is obtained by an interplay of various properties of the absorber such as chemical composition, morphology, particle size and its distribution in a cermet composition. Furthermore, interference effects obtained in a suitably stacked layer structure also contribute to selectivity. Examples of many such absorbers are available in the literature [1, 2]. Therefore, it is very important to characterize the absorber chemically and physically to explain the optical selectivity.

In our earlier communication [3] we have described the method of preparation by standardizing the electrochemical parameters to obtain reproducible, adherent molybdenum-black films with good solar selectivity. We have also reported preliminary results on characterization of these films.

In this paper we report the properties of these films. It is shown that reflectance in the infrared (IR) is due to the metal substrate used for the deposition of the films, and the absorption mechanism in the visible and near-IR is quite complicated. A simple Maxwell Garnett (MG) theory does not explain the absorption properties of our films. It is shown that only by postulating a stacked layer structure for the film and then applying the MG theory, could we obtain the calculated absorption in the visible-near IR (VIS-NIR) region close to that obtained experimentally in our films.

## 2. Experimental procedure

The films were prepared by using a bath of: (1) nickel sulphate ( $\text{NiSO}_4$ ),  $144 \text{ g l}^{-1}$ , (2) ammonium molybdate ( $(\text{NH}_4)_2\text{MoO}_4$ ,  $30 \text{ g l}^{-1}$ , (3) boric acid ( $\text{H}_3\text{BO}_3$ ),  $22.5 \text{ g l}^{-1}$ , (4) copper sulphate ( $\text{CuSO}_4$ ),  $2 \text{ g l}^{-1}$ .

The standardised parameters used were: temperature of the bath, 35 to 45°C; current density,  $4 \text{ mA cm}^{-2}$ ; deposition time, 60 sec; distance between two electrodes 4.5 cm; cathode  $2 \text{ cm} \times 6 \text{ cm}$  nickel-plated copper strip; anode  $2 \text{ cm} \times 6 \text{ cm}$  copper strip with thick nickel plating; voltage across the two elec-

trodes, 2.5 to 3 V. Both the electrodes were polished and cleaned, steps which are essential for obtaining reproducible, adherent films. A few films were deposited on the substrate without using copper sulphate in the bath, the result of which is discussed later.

### 2.1. Reflectance measurement

The reflectance measurements in the range 0.4 to  $0.8 \mu\text{m}$  were taken using a spectrophotometer [4] designed and fabricated in this laboratory. Total reflectance of these films was recorded as a function of wavelength in the region 0.38 to  $0.76 \mu\text{m}$  with a Pye Unicam spectrophotometer model UV/VIS SP8-100 using the reflectance attachment. Normal reflectance measurement in the region 1 to  $15 \mu\text{m}$  was taken using a Perkin Elmer double-beam spectrophotometer model 221 using the reflectance attachment.

Solar absorptance ( $\alpha$ ) and thermal emittance ( $\epsilon$ ) were measured using the D and S (Devices and Services Co.) alphanometer and emissometer, respectively.

X-ray diffraction study was carried out using a Philips PW 1730 diffractometer with  $\text{CuK}\alpha$  radiation. A Cambridge stereo scan 150 microscope was used to study the surface morphology of the films. Chemical composition of these films was measured using X-ray photoelectroscopy (XPS) and Auger electron spectroscopy (AES). XPS spectra of these films were recorded on a Vacuum Generator's instrument model ESCA-3M-KII using  $\text{MgK}\alpha$  (1253.6 eV) or  $\text{AlK}\alpha$  (1486.6 eV) as the radiation source. Films were coated with a thin layer of gold or aluminium to avoid charging effects and to provide an internal reference. AES was recorded on the above instrument using an electron beam for excitation. Using the sputtering facility provided with the instrument, the AES depth profiling was carried out. A differentially pumped argon ion gun with 0 to 10 kV energy was used for sputter-etching. During the AES depth profile studies, the peak-to-peak height of Auger peaks was measured as a function of sputtering time.

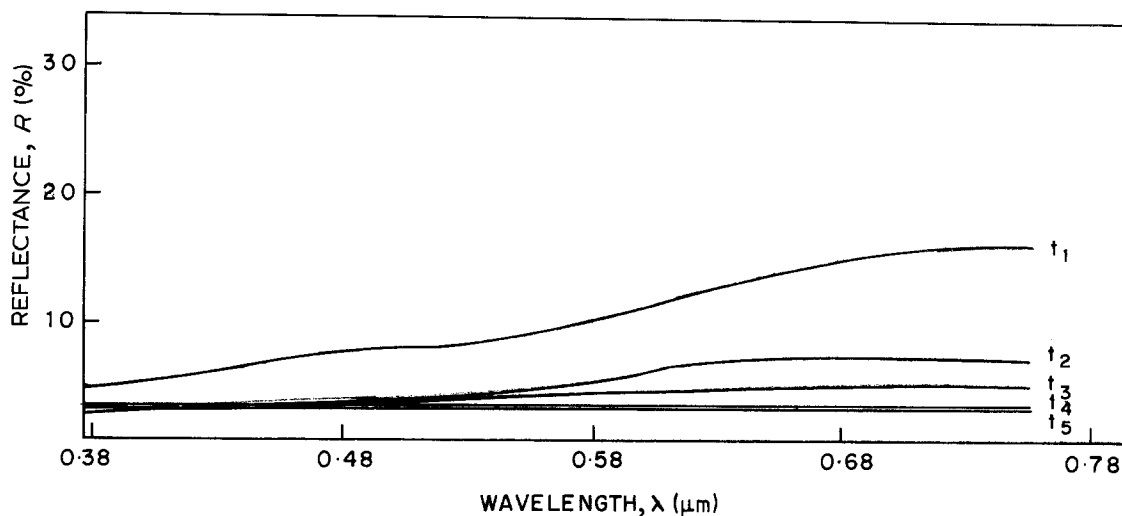


Figure 1 Effect of deposition time on the total reflectance of the molybdenum-black film.  $t_1 = 30$  sec,  $t_2 = 45$  sec,  $t_3 = 60$  sec,  $t_4 = 75$  sec,  $t_5 = 100$  sec.

## 2.2. Chemical analysis

The standard chemical analysis techniques were used to determine the film composition.

## 3. Results and discussion

Figs 1 and 2 show the effect of deposition time on reflectance in the regions 0.38 to 0.76  $\mu\text{m}$  and 1 to 15  $\mu\text{m}$ . The time of 60 sec is optimized for high absorption in the solar region with low emittance in the IR region. The resulting selectivity for the film deposited at time  $t = 60$  sec is shown in Fig. 3. For comparison, Fig. 3 also shows the reflectance of the substrate and that of the film prepared without using  $\text{CuSO}_4$  in the bath.

It is interesting to note the following points from Fig. 3. (i) The film prepared without addition of  $\text{CuSO}_4$  to the bath has a poor selectivity. (ii) There is a definite improvement in the selectivity on addition of  $\text{CuSO}_4$  to the bath. (iii) There are two peaks, one in the VIS-NIR and the other in the IR region. The former is perhaps due to interference effects and the latter to characteristic absorption by the vibrational mode of adsorbed water.

The values of  $\alpha$  and  $\epsilon$  were calculated to be 0.85 and 0.11, respectively, as reported earlier [3]. The absorbance,  $\alpha = 0.85$ , computed from the reflectance measurement is in good agreement with absorbance (0.86) measured using an alphanometer. These selective films were used for further characterization.

### 3.1. Structure and morphology of the films

X-ray diffraction and electron diffraction studies revealed that the films are non-crystalline in nature. An attempt was made to crystallize these films by heating up to 350°C for 7 h. The X-ray diffraction study of the heated film showed that the  $d$  values matched those reported for the  $\text{Mo}_4\text{O}_{11}$  phase. The typical surface microstructure of the film deposited at optimized time  $t = 60$  and 100 sec is shown in Figs 4 and 5, respectively. It is seen from these figures that the particle size in films deposited for 60 sec is of the order of 0.1 to 0.5  $\mu\text{m}$ . The particle size increases with deposition time and in the samples deposited for  $t = 100$  sec, the particle size is  $\geq 1 \mu\text{m}$ . It may also be noted that the particles are generally spherical in shape, and there is less clustering in the films deposited

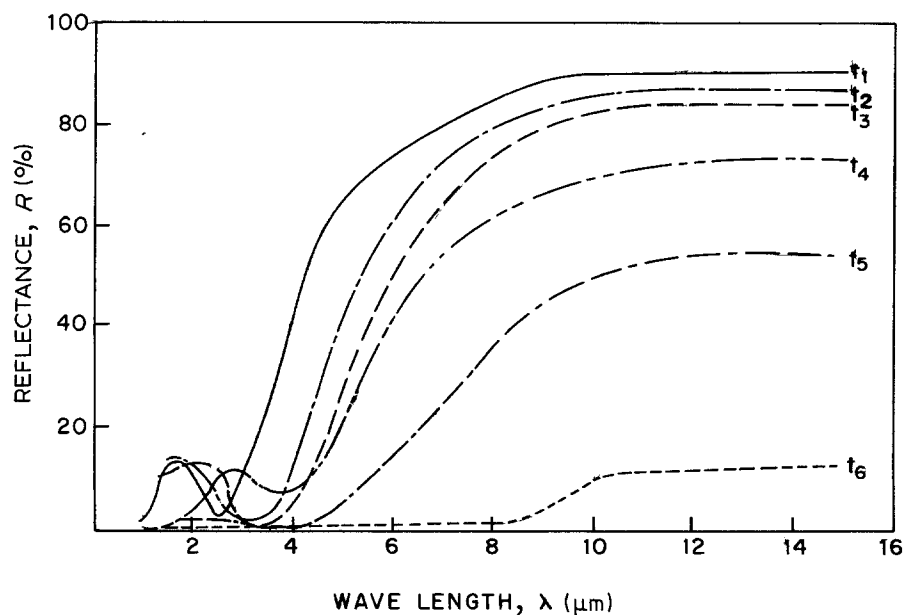


Figure 2 Effect of deposition time on IR reflectivity of the molybdenum-black film.  $t_1 = 30$  sec,  $t_2 = 45$  sec,  $t_3 = 60$  sec,  $t_4 = 65$  sec,  $t_5 = 75$  sec,  $t_6 = 100$  sec.

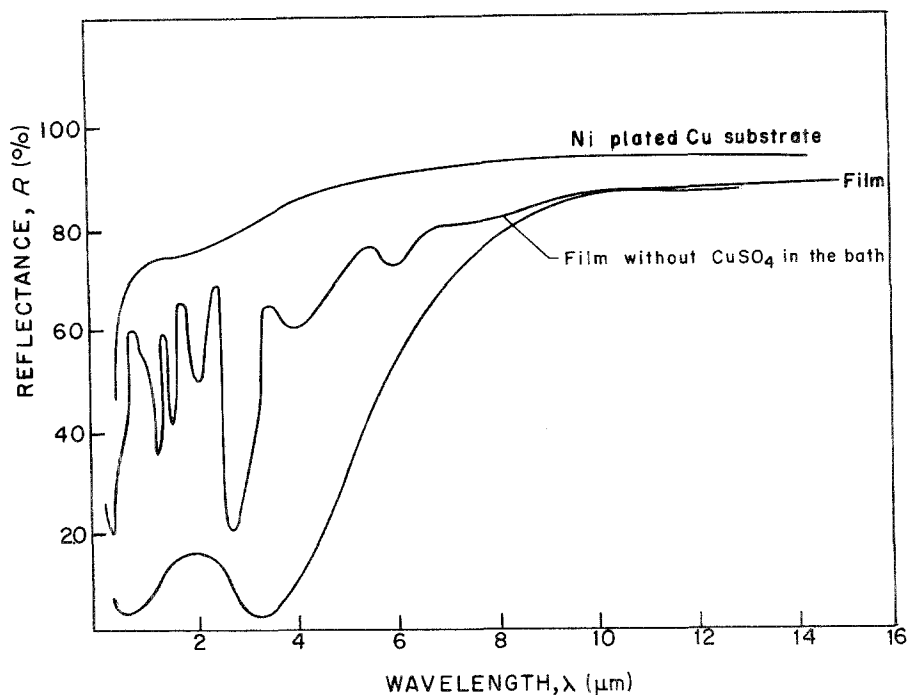


Figure 3 Reflectance ( $R$ ) as a function of wavelength,  $\lambda$ , of the selective molybdenum-black film and nickel-plated copper substrate.

for 60 sec compared to those obtained after 100 sec. The porous nature of the film deposited at  $t = 60$  sec is evident from the small voids seen in the photograph.

### 3.2. Chemical analysis

Atomic absorption spectroscopy and gravimetry were employed to determine the volume fractions of copper, nickel and  $\text{MoO}_3$ . The respective bulk densities were taken from the literature [6]. The results are: volume fraction of copper = 0.32, volume fraction of nickel = 0.01, volume fraction of  $\text{MoO}_3$  = 0.67.

### 3.3. XPS and AES

XPS of the as-prepared selective molybdenum-black film is shown in Fig. 6a. An intense peak is seen at 232.2 eV which is assigned to  $\text{Mo}3d_{5/2}$ . The peak at 235.4 eV is due to  $\text{Mo}3d_{3/2}$ , and the intensity ratio is 1.5. These observations are in good agreement with the values reported for  $\text{MoO}_3$  [6], and suggest that up to the penetration depth of X-rays the film contains  $\text{Mo}^{6+}$  state only. The peaks at 932.8 and 853.6 eV are assigned to  $\text{Cu}2p_{3/2}$  and  $\text{Ni}2p_{3/2}$  respectively. The binding energy (BE) of nickel matches that reported for the  $\text{Ni}(0)$  state [7] while the BE corresponding to the

copper XPS peak matches the reported value of the  $\text{Cu}(0)$  or of  $\text{Cu}(I)$  state [8, 9].

The AES study of the virgin sample (Fig. 7) gave a doublet structure with peak positions at 186 and 182.6 eV ( $M_{45}N_{23}V$  transition). The intense peak at 182.6 eV is attributed to the 6+ oxidation state of molybdenum and the less intense peak at 186 eV is assigned to the  $\text{Mo}^{4+}$ -oxidation state. These values were found to be in agreement with the reported values for those species [10, 11]. While XPS of the same sample did not show a peak corresponding to the  $\text{Mo}^{4+}$  oxidation state, it is shown by AES due to the reduction by electron-beam exposure [10]. It may be noted that no signals for copper or nickel in any of their oxidation states were observed in AES having less penetration depth than XPS. This leads us to conclude that the top layer consists of pure  $\text{MoO}_3$  without any additives. However, XAES of the film gave a peak at  $\text{KE} = 919.0$  eV which agrees with that reported for the  $\text{Cu}(0)$  state [8, 9]. From the above observations, it can be concluded that the film is made up of an  $\text{MoO}_3$  matrix containing nickel and copper in the metallic state.

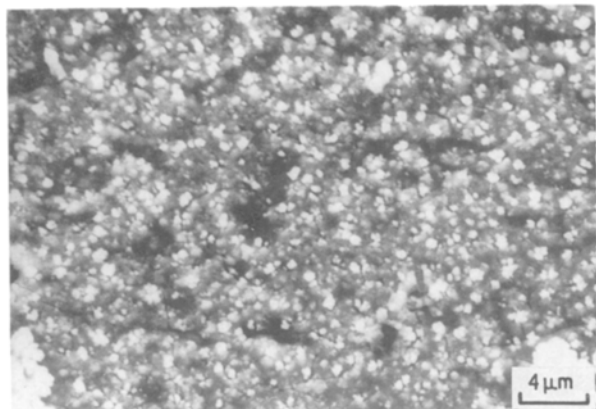


Figure 4 Scanning electron micrograph of selective molybdenum-black film.

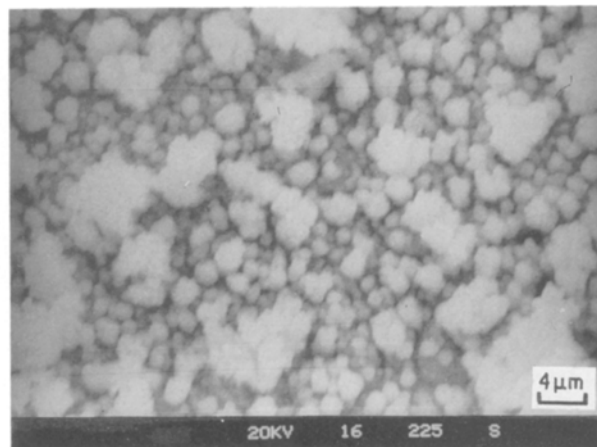


Figure 5 Scanning electron micrograph of thicker (nonselective) molybdenum-black film.

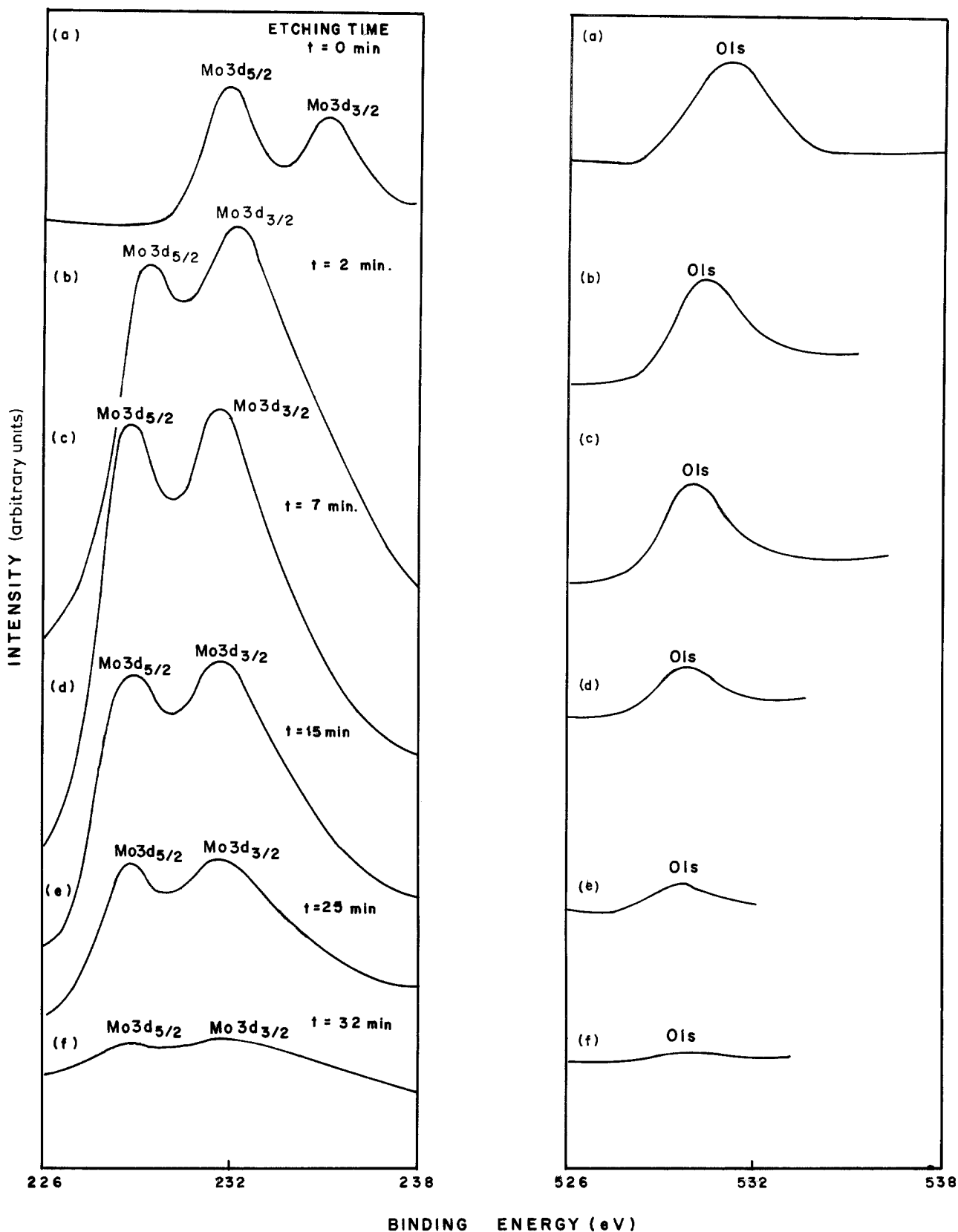


Figure 6 XPS of selective molybdenum-black film after successive etchings for molybdenum, oxygen, copper and nickel: (a) as-prepared, (b, c, d, e, f) after etchings with the argon-ion gun.

The XPS of selective molybdenum-black film after successive etchings are shown in Figs 6b, c, d, e and f. The following changes in the XPS may be noted: (i) A new peak appears at 229 eV. (ii) The peak in the region of 232 eV is broadened while its intensity increases. (iii) The position and intensity of peaks assigned to Ni(0) and Cu(0) remain nearly the same down to the substrate. (iv) The oxygen (O1s) peak intensity is

lowered on going down from the surface of the film to the bottom, although its position remains unchanged.

The spectrum obtained after the first etching has been resolved manually (Fig. 8) using the reported data [6] Mo (4+)  $3d_{5/2}$  = 229.4 eV, Mo (6+)  $3d_{5/2}$  = 232.5 eV, Mo (5+)  $3d_{5/2}$  = 231.0 eV, splitting between  $3d_{5/2}$  and  $3d_{3/2}$  = 3 eV, FWHM = 2.3 eV.

It is found that the fitting of the resolved spectrum

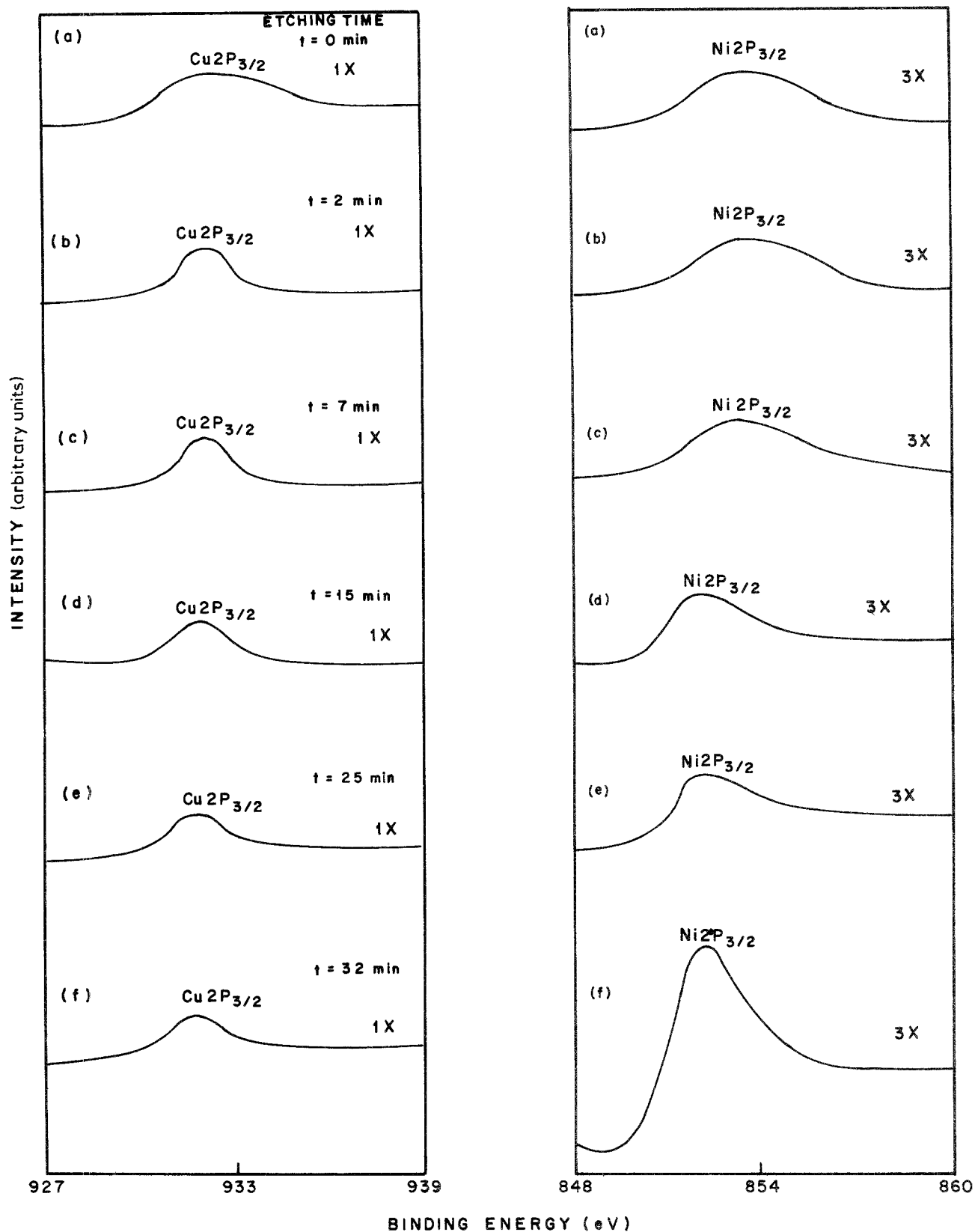


Figure 6 Continued.

is possible by considering Mo<sup>4+</sup>, Mo<sup>5+</sup> and Mo<sup>6+</sup> species to be present after etching of the sample. This is in agreement with the reported argon-ion reduction of Mo<sup>6+</sup> to Mo<sup>5+</sup> and Mo<sup>4+</sup> by Kim and co-workers [7, 12]. If Mo<sup>5+</sup> and Mo<sup>4+</sup> species have resulted from the argon-ion reduction process only, then it can be concluded that the virgin film contains only Mo<sup>6+</sup> throughout the bulk. To confirm the above conclusion, and to rule out the possibility that the as-prepared selective film may have Mo<sup>4+</sup>, Mo<sup>5+</sup> in

addition to the Mo<sup>6+</sup> species in the bulk, the XPS of the film was studied after etching out the top layer of the film with dilute HCl. The XPS is shown in Fig. 9 and it is interesting to note that all the features of the as-prepared sample are reproduced. Pure MoO<sub>3</sub> showed the same observations in XPS [13], both in the pure state and after etching which gives additional support to the conclusion that our virgin film consists of Mo in the 6<sup>+</sup> state only. An examination of the intensity of molybdenum and copper XPS peaks after

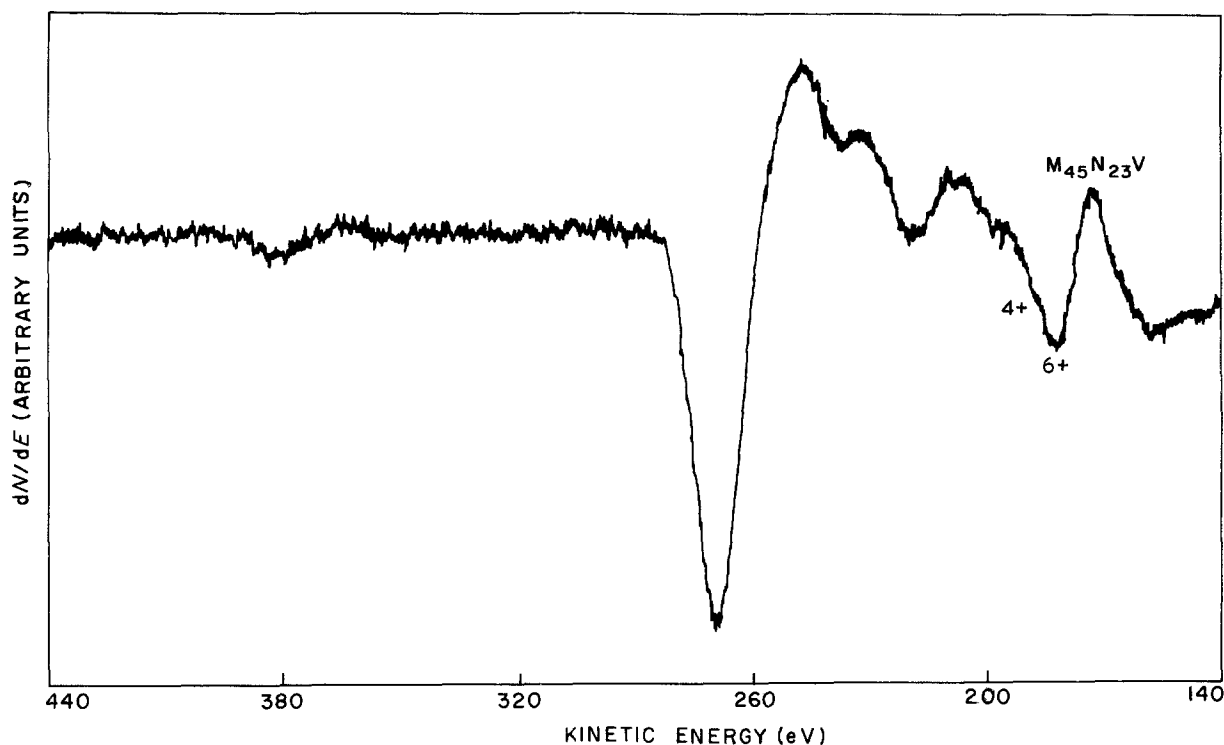


Figure 7 AES of a selective molybdenum-black film on a 440 to 140 eV kinetic energy scale.

successive etchings reveals the following features. (i) The intensity of the copper peak remains the same throughout the etching process. (ii) Up to the third etching (etching time = 7 min) the molybdenum peak intensity keeps increasing. (iii) After the third etching the molybdenum intensity decreases.

As the molybdenum intensity increases up to an etching time of 7 min, one can conclude that the top layer of the film contains  $\text{MoO}_3$  without metal particles in it. The copper and nickel signals are obtained because of the porous nature of the films as revealed earlier by SEM studies. Also, we feel that the porous nature increases with film thickness and therefore one can expect an increase in the molybdenum signal on

studying the XPS from the top towards the substrate. Simultaneously, if the first and third observations are considered together, one can state that the Mo/Cu ratio decreases along the bulk towards the substrate. In other words, the volume fraction of 0.32 is not uniform in the bulk, but shows a gradual decrease from surface to substrate. This observation further supports our suggestion that after a certain layer thickness, there is a layer of  $\text{MoO}_3$  containing no copper. The AES profile is shown in Fig. 10: it indicates that the peak-to-peak height ratio for O/Mo is 2.8 at the surface, but it changes to 2 after etching and then remains more or less constant up to the substrate. This observation can be explained by considering the presence of the  $\text{Mo}^{6+}$  state throughout the bulk. After etching,  $\text{Mo}^{6+}$  is converted to  $\text{Mo}^{4+}$  and  $\text{Mo}^{5+}$  because of argon-ion reduction [11] and electron-beam exposure [10], thus reducing the O/Mo ratio. This is consistent with the XPS, AES studies discussed earlier.

It should be noted that even at the surface, the O/Mo ratio obtained is less than expected for  $\text{MoO}_3$  [1]. This is reasonable because the films are formed at the cathode where some reduction is likely to occur. This is also consistent with X-ray results of the heated sample where the defect structure of  $\text{MoO}_3$ , i.e.  $\text{Mo}_4\text{O}_{11}$ , is shown for which the O/Mo ratio is expected to be 2.75.

### 3.4. Optical properties

The properties investigated from the reflectance-wavelength curve are (i) low reflectance in the solar region or measured high  $\alpha = 0.85$ , and (ii) high reflectance or measured low  $\epsilon = 0.11$  in the IR region of the spectrum. The high reflectance in the IR region can be explained on the basis of reflectance from the metal substrate. Fig. 3 shows the reflectance of the film

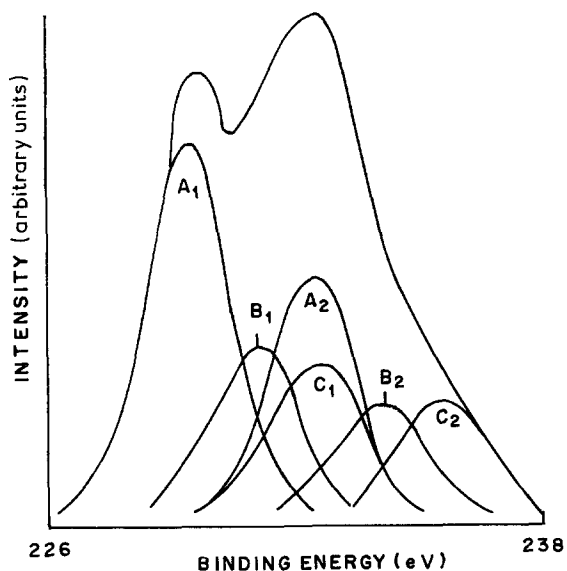


Figure 8 XPS of molybdenum-black film after the first etching with resolved peaks.  $A_1$ ,  $3d_{5/2}(\text{Mo}^{4+})$ ;  $A_2$ ,  $3d_{3/2}(\text{Mo}^{4+})$ ;  $B_1$ ,  $3d_{5/2}(\text{Mo}^{5+})$ ;  $B_2$ ,  $3d_{3/2}(\text{Mo}^{5+})$ ;  $C_1$ ,  $3d_{5/2}(\text{Mo}^{6+})$ ;  $C_2$ ,  $3d_{3/2}(\text{Mo}^{6+})$ .

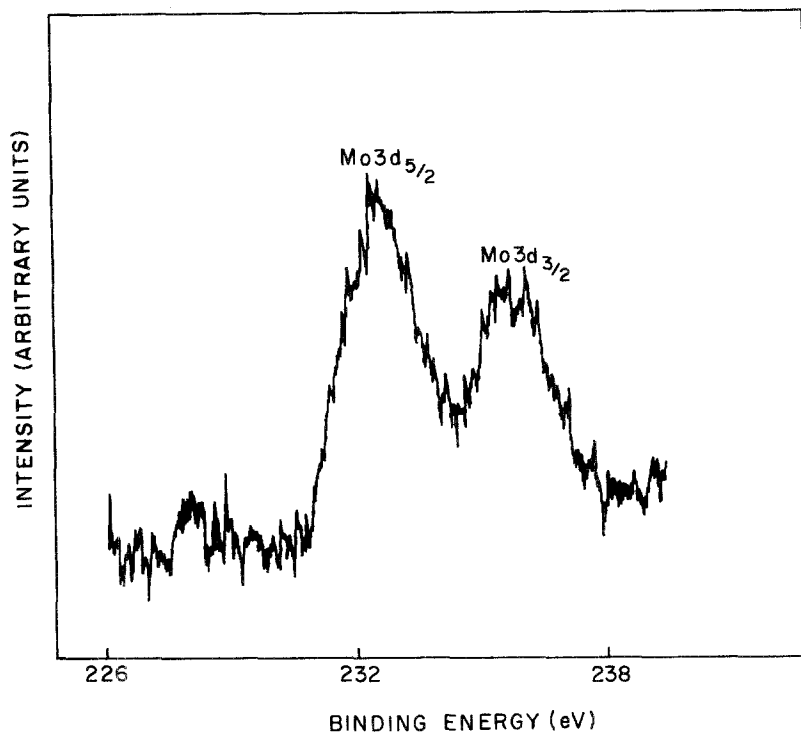


Figure 9 XPS of selective molybdenum-black film after treating with HCl.

and that of the metal substrate without the film which are comparable taking into account some losses due to the film over the substrate. For such a reflectance observation, it is necessary that the film over the substrate is transparent for this region of the spectrum. The band gap of  $\text{MoO}_3$  is 3.4 to 3.5 eV [14, 15], which makes it transparent for all wavelengths beyond the absorption edge.

To explain the high absorption, we considered various possibilities based upon our physical and chemical characterization. There are reports in the literature that dielectric films dispersed with metal particles can have absorption according to MG theory or its modifications [15–20]. We propose application of this theory because the requirements are fulfilled, i.e. (i) matrix having a high dielectric constant [14, 15] ( $\text{MoO}_3 = 6.13$ ) dispersed with (ii) metal particles, which are spherical, and (iii) the critical volume fraction of the components requirement depending upon the system in which the metal volume fraction is lower than the matrix; in the present case, copper volume

fraction = 0.32,  $\text{MoO}_3$  volume fraction = 0.67, and nickel volume fraction = 0.01. The nickel volume fraction is small (0.01) and calculations showed that it has negligible contribution towards the high  $\alpha \approx (0.85)$  found in our samples. Therefore, we considered our layers to be a composite of copper particles in an  $\text{MoO}_3$  matrix for calculations of  $\alpha$ .

Theoretical curves based on the MG theory showing variation of reflectance with  $\lambda$  for copper in  $\text{MoO}_3$  are shown in Fig. 11. It can be seen that the observed absorption in the solar region in our experimental curves is partly explained by considering the  $\text{Cu}/\text{MoO}_3$  composite, as it shows a high absorption in the visible part of the spectrum. This shows clearly that the absorption is brought about by the  $\text{Cu}/\text{MoO}_3$  composite with some other mechanism in addition to the MG theory. We decided to use the  $\text{MoO}_3$  layer without any additives covering the  $\text{Cu}/\text{MoO}_3$  composite. Such layered stacks increase the absorption as shown by Anderson [21]. We propose the following model based on our experimental observations (Fig. 12).

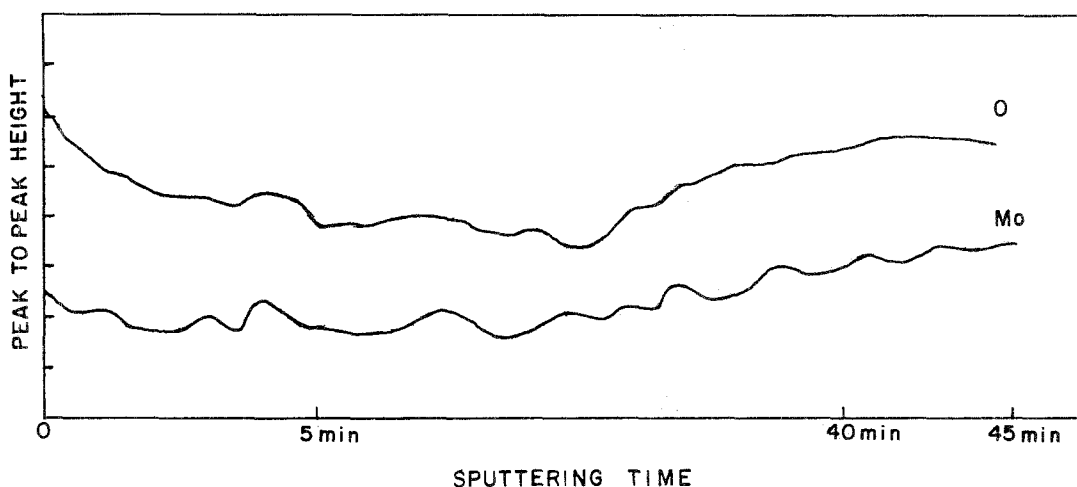


Figure 10 AES depth profile of selective molybdenum-black film.

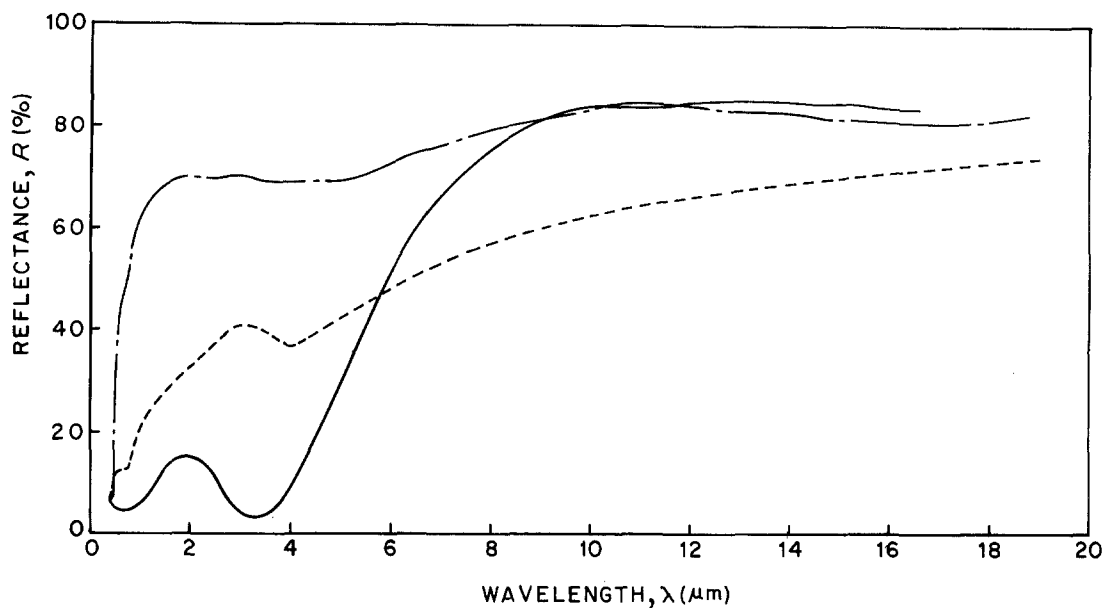


Figure 11 Reflectance ( $R$ ) as a function of wavelength,  $\lambda$ , of the selective molybdenum-black film. (—) Experimental, (---) calculated using MG theory, (···) calculated using MG and Anderson's treatment.

The reflectance ( $R$ ) of the stack is given by

$$R = \frac{|A - C + (B - D)N_s|^2}{|A + C + (B + D)N_s|^2}$$

where  $N_s$  is the refractive index of the substrate at a particular wavelength, A, B, C and D are the elements of the transfer matrix  $M$  given by

$$M_i = \prod_1^2 M_i = \begin{pmatrix} A & B \\ C & D \end{pmatrix}$$

where

$$M_i = \begin{pmatrix} \cos \xi_i & -i/N_i \sin \xi_i \\ -iN_i \sin \xi_i & \cos \xi_i \end{pmatrix}$$

where  $\xi_i = 2\pi N_i t_i / \lambda$ ,  $N_i = \epsilon_i^{1/2}$ , where  $\epsilon_i$  is the dielectric constant and  $t_i$  is the thickness of the  $i$ th layer.

Referring to the Fig. 11, the effect of pure  $\text{MoO}_3$  over  $\text{Cu}/\text{MoO}_3$  tandem shows that there is a flat absorption in the solar region compared to that obtained by the MG theory alone. The calculated reflectance-wavelength curve is close to that obtained experimentally, except for the sharp absorption peak around  $2.5 \mu\text{m}$  which we attribute to the vibrational mode of water adsorbed during electrochemical deposition. The additional proof for this is obtained in our stability studies in which it is observed that selec-

tive films heated at 100, 200 and  $300^\circ\text{C}$  show successive lowering of absorption at  $2.5 \mu\text{m}$  attributed to adsorbed water. The details of stability and degradation studies will be published later.

For calculations of the stacked layer tandem we have presumed that the layer has uniform dielectric constants although the  $\text{Cu}/\text{MoO}_3$  layer will have continuously changing  $\epsilon$  because of the increasing concentration of copper towards the substrate. If we take this approximation into account, the agreement in the experimental and theoretical curves is very reasonable. In fact, the agreement would improve if one introduces the variation of dielectric constant ( $\epsilon_i$ ) with thickness into calculations.

#### 4. Conclusions

Solar-selective molybdenum-black films deposited by a cathodic electrodeposition technique consist of an  $\text{MoO}_3$  matrix containing fine spherical copper and nickel particles in the metallic state. The MG theory together with the stacked layers treatment used by Anderson show that the optical properties for the films are comparable to those observed experimentally.

#### References

1. O. P. AGNIHOTRI and B. K. GUPTA, "Solar Selective Surfaces" (Wiley, New York, 1981).

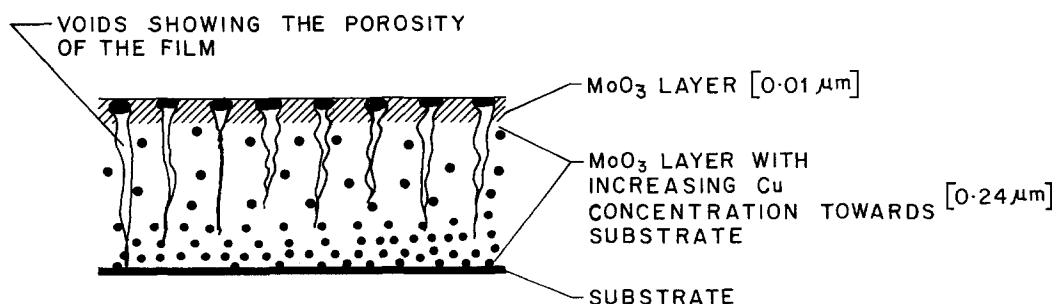


Figure 12 Proposed model for selective molybdenum-black film.



2. G. A. NIKLASSON and C. G. GRANQVIST, *J. Mater. Sci.* **18** (1983) 3475.
3. H. S. POTDAR, R. I. HEGDE, S. BADRINARAYANAN and N. R. PAVASKAR, *Solar Energy Mater.* **6** (1982) 183.
4. A. GOSWAMI and B. V. RAO, *Ind. J. Pure Appl. Phys.* **12** (1974) 21.
5. J. W. MELLOR, "A Comprehensive Treatise on Inorganic and Theoretical Chemistry", Vols. III and XI (Longman, London).
6. W. E. SWARTZ, Jr. and D. M. HERCULES, *Anal. Chem.* **43** (1971) 1774.
7. K. S. KIM and W. E. BAITINGER, J. W. AMY and N. WINOGRAD, *J. Electron. Spectrosc. Relat. Phenom.* **5** (1974) 351.
8. G. SCHON, *Surf. Sci.* **35** (1973) 96.
9. PAUL E. LARSON, *J. Electron. Spectrosc. Rel. Phenom.* **4** (1974) 213.
10. T. T. LIN and DAVID LITCHMAN, *J. Vac. Sci. Technol.* **15** (1978) 1689.
11. L. E. FIRMAT and A. FERRETTI, *Surf. Sci.* **129** (1983) 155.
12. K. S. KIM and NOCHOLAS WINOGRAD, *Surf. Sci.* **43** (1974) 625.
13. H. S. POTDAR, PhD thesis, University of Poona (1984), submitted.
14. A. A. HANNA and M. A. KHILLA, *Thermochim. Acta* **65** (1983) 311.
15. R. B. DZHANELIDZE, I. M. PURTSELADZE, L. S. KHITARISHVILI, R. I. CHIKOVANT and A. L. SHKOL'NIK, *Sov. Phys. Solid State* **7** (1966) 2082.
16. H. G. CRAIGHEAD, R. BARTYNSKI and R. BUHRMAN, *Solar Energy Mater.* **1** (1979) 105.
17. J. C. C. FAN and S. A. SPURA, *Appl. Phys. Lett.* **30** (1977) 511.
18. D. R. MCKENZIE, *Thin Solid Films* **62** (1979) 317.
19. J. C. C. FAN and P. M. ZAVRACKY, *Appl. Phys. Lett.* **29** (1976) 48.
20. A. J. SIEVERS, *Topics Appl. Phys.* **31** (1979) 111.
21. A. ANDERSON, *J. Appl. Phys.* **51** (1980) 754.

*Received 22 April  
and accepted 23 September 1986*